

One-loop unquenched three-gluon vertex in the Curci-Ferrari model

Felipe Figueroa

*Laboratoire d'Annecy-le-Vieux de Physique Théorique LAPTh, Université Grenoble Alpes,
Université Savoie Mont Blanc, CNRS, F-74000 Annecy, France*

Marcela Peláez

Instituto de Física, Facultad de Ingeniería, Universidad de la República, Montevideo, Uruguay

(Dated: October 20, 2021)

In this article we study the unquenched three-gluon vertex in all momentum range going from the ultraviolet to the infrared regime using the Curci-Ferrari model at one-loop in Landau gauge as an extension of the results presented in [1]. Results are compared with recent lattice data for $SU(3)$ in the unquenched case. This calculation is a pure prediction of the model because it does not require fixing any parameter once two-point functions are fitted. An analysis of the influence of dynamical quarks in the position of the zero crossing is presented. Due to the recent improvement of infrared lattice data for the quenched three-gluon correlation function [2] we also redo the comparison of one-loop results in this limit obtaining very good results.

I. INTRODUCTION

The infrared sector of QCD is usually called the Non-perturbative regime due to the fact that standard perturbation theory based on Faddeev-Popov Lagrangian presents a Landau pole in the infrared. This implies that perturbation theory cannot be applied together with this particular gauge-fixed Lagrangian to study the infrared. For these reasons different alternatives have been developed in order to approach this regime. These approaches can be classified in two different categories, the first one includes non-perturbative functional techniques, for instance, treatments based on Schwinger-Dyson (SD) [3–18] or Non perturbative renormalization group (NPRG) equations [19–25]. The other category includes approaches that focus on finding the correct gauge-fixed Lagrangian that should be used in the infrared. This line is motivated due to the fact that Faddeev-Popov procedure, generally used to fix the gauge, is not completely justified in the infrared because of Gribov copies [26]. Therefore, until now it is not known how to build from first principles the correct gauge-fixed Lagrangian valid in the infrared. There are some interesting attempts to reach this Lagrangian based on Gribov-Zwanziger action and the refined Gribov-Zwanziger approach [27–29].

Lattice simulations can deal with the problem of Gribov copies so they are a good tool to obtain information about the infrared behavior of Yang-Mills theory. Two important observations of lattice simulations are, first, that the gluon propagator behaves as a massive propagator in the infrared [30–37]. Second, that the relevant expansion parameter obtained through the ghost-gluon or the three-gluon vertex does not present a Landau-pole and in fact it does not become too large [33, 38–40]. These points have motivated us to study the infrared regime using a gauge-fixed Lagrangian with a gluon mass term [41, 42]. This Lagrangian is a particular case of Curci-Ferrari Lagrangians in Landau gauge (CF) [43].

Even though we do not know how to justify CF Lagrangian from first principles it is important to observe

that it can reproduce a great variety of correlation functions using the first order in perturbation theory. It is important to mention that we do not dare to try to reproduce all infrared quantities of QCD perturbatively, in particular the perturbative expansion for correlation functions involving quarks near the chiral limit fails. Other approach using CF model was proposed in [44, 45] in order to explore the chiral limit. See [46] for a detail summary of the already studied properties of the model. In particular, one-loop corrections within the CF model were computed for propagators, ghost-gluon vertex and the quenched three-gluon vertex [1, 42, 47–49]. In addition to this, two-loop corrections were studied for propagators [50, 51] and the ghost-gluon vertex with a vanishing gluon momentum [52] and compared with lattice data with great accuracy. It is important to mention that vertices are obtained as a pure prediction of the model, in the sense that the free parameters are fixed by minimizing the error between propagators and the corresponding lattice data and therefore there are no free parameters left when studying vertices.

The aim of this article is to extend the study of one-loop corrections for the three gluon vertex in the presence of dynamical quarks. The infrared regime of the three-gluon vertex has been studied by different approaches specially in the last decade [1, 16, 24, 53–69] as it is an important ingredient to understand QCD at low energies. The three-gluon vertex is more difficult to calculate than the propagators because instead of depending on a single momentum, it depends on three independent scalars. Moreover, it has a richer tensorial decomposition so different scalar functions (associated with different tensors) have to be reproduced together.

In this article, we study the effects of dynamical quarks in the three-gluon vertex using one-loop CF model. The unquenched results are compared with lattice data from [70]. Moreover, recent simulations of the quenched three-gluon vertex show a better handling of the infrared regime, yielding more precise data in this limit [2]. For this reason it is worth to extend the results presented in

[1] for $SU(2)$ to $SU(3)$ gauge-group and compare it with the newest lattice data. For both cases, quenched and unquenched, the parameters used in the plots were chosen to minimize the error of the propagators previously computed in [47, 50]. In this sense, the results shown in this article are a pure prediction of the model that reproduces with great accuracy the lattice data. Due to the presence of massless ghosts, CF model also features a zero crossing as it is observed in [56, 62, 65–68]. We also find that dynamical quarks shift the zero crossing in a direction that depends on the momentum configuration in a way consistent with what is observed in [60].

The article is organized as follows. In Sec. II we describe in more detail the Curci-Ferrari model in Landau gauge. We give some details on the one-loop calculations of the three-gluon vertex in Sec. III in terms of the Ball-Chiu components. In Sec. IV we present the renormalization conditions and the renormalization group equations. We present our results in Sec. V. and compare them with lattice data. At the end of the article we present the conclusions of the results.

II. CURCI-FERRARI MODEL WITH QUARKS

We start by introducing the Curci-Ferrari Lagrangian [43] in the presence of dynamical quarks in Euclidean space:

$$\begin{aligned} \mathcal{L} = & \frac{1}{4}(F_{\mu\nu}^a)^2 + \partial_\mu \bar{c}^a (D_\mu c)^a + ih^a \partial_\mu A_\mu^a \\ & + \frac{m^2}{2}(A_\mu^a)^2 + \sum_{i=1}^{N_f} \bar{\psi}_i (\gamma_\mu D_\mu + M_i) \psi_i, \end{aligned} \quad (1)$$

where g is the coupling constant, and the flavor index i spans the N_f quark flavors.

The covariant derivative D_μ acting on a ghost field in the adjoint representation of $SU(N)$ reads $(D_\mu c)^a = \partial_\mu c^a + gf^{abc} A_\mu^b c^c$, while when applied to a quark in the fundamental representation it reads $D_\mu \psi = \partial_\mu \psi - gt^a A_\mu^a \psi$. The latin indices correspond to the $SU(N)$ gauge-group, the t^a are the generators in the fundamental representation and the f^{abc} are the structure constants of the group. Finally, the field strength is given by $F_{\mu\nu}^a = \partial_\mu A_\nu^a - \partial_\nu A_\mu^a + gf^{abc} A_\mu^b A_\nu^c$.

The Feynman rules associated to this Lagrangian are the standard Feynman rules for Euclidean-QCD in Landau gauge except for the gluon's free propagator, which reads

$$\langle A_\mu^a A_\nu^b \rangle_0(p) = \delta^{ab} P_{\mu\nu}^\perp(p) \frac{1}{p^2 + m^2}, \quad (2)$$

where we have introduced the transverse projector:

$$P_{\mu\nu}^\perp(p) = \delta_{\mu\nu} - \frac{p_\mu p_\nu}{p^2}. \quad (3)$$

It is important to mention that the gluon mass term added to the Faddeev-Popov Lagrangian breaks the BRST symmetry. However, it can be shown that (1) satisfies a modified (non-nilpotent) BRST symmetry that can be used to prove its renormalizability [71].

Probably the most interesting aspect of this model is the fact that, as it has been shown in various previous articles (see [41, 42, 49, 50, 77] for instance), the addition of a gluon mass term regularizes the theory in the infrared, allowing for a perturbative treatment of the theory in this region. More specifically, it is possible to find a renormalization scheme without an infrared Landau pole for particular choices of the initial condition of the renormalization-group flow. These features have made it possible to use this model to compute various two and three-point functions to 1-loop and 2-loop order, obtaining a very good match with lattice simulations [1, 42, 47, 48, 50–52]. It is important to mention that this model has also been studied at finite temperature and chemical potential in [72–74].

III. ONE-LOOP CALCULATION OF THE THREE GLUON VERTEX

A. Tensorial structure and computation

In this work we extend the one-loop computation of the gluon three-point function obtained in [1] for $SU(N)$ Yang-Mills theory to unquenched QCD. In order to calculate the gluon's three-point function at one-loop order we need to compute the Feynman diagrams shown in Fig 1.

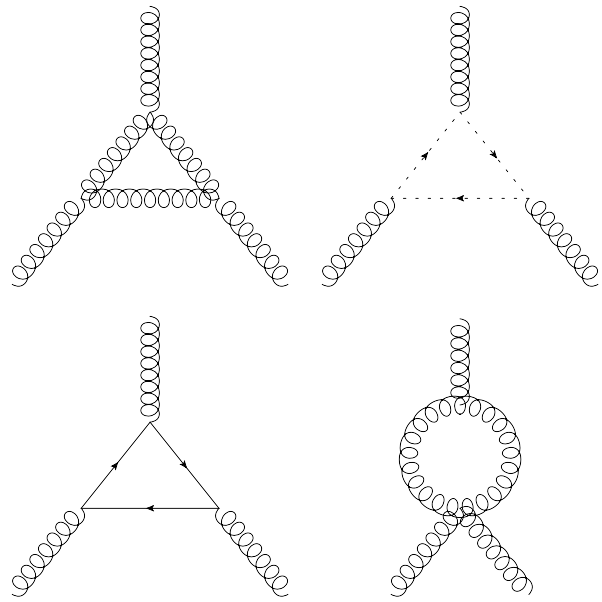


FIG. 1. Feynman diagrams present in the one-loop calculation of the three-gluon vertex.

As shown in [75], the color structure of the three-gluon

vertex is simply the structure constant f^{abc} of the $SU(N)$ group, so it can be factored out. Furthermore, we follow the usual convention [76] of factorizing the coupling constant, and thus we define:

$$\Gamma_{A_\mu^a A_\nu^b A_\rho^c}^{(3)}(p, k, r) = -igf^{abc}\Gamma_{\mu\nu\rho}(p, k, r)$$

The tensor structure of $\Gamma_{\mu\nu\rho}(p, k, r)$ can be easily deduced: it must depend on three Lorentz indices (one for each gluon) and on two independent momenta due to momentum conservation. As a consequence, we can have only two types of tensor structures: the ones made up of

three momenta ($p_\mu p_\nu p_\rho, p_\mu p_\nu k_\rho, \dots$) and the ones made up of one momentum and the Euclidean metric tensor ($p_\mu \delta_{\nu\rho}, k_\nu \delta_{\mu\rho}, \dots$). It's not hard to convince oneself that there are eight possible terms of the first kind and six of the second, adding up to a total of 14 possible terms in the vertex's tensor structure. However, the vertex is symmetric under the exchange of any pair of external legs, and this ends up reducing the total number of possible independent coefficients in the vertex's tensor structure to six.

A cleaner way of exploiting these symmetries is following the decomposition proposed by Ball and Chiu in [78], where they parametrize the vertex using six scalar functions:

$$\begin{aligned} \Gamma_{\mu\nu\rho}(p, k, r) = & A(p^2, k^2, r^2)\delta_{\mu\nu}(p-k)_\rho + B(p^2, k^2, r^2)\delta_{\mu\nu}(p+k)_\rho - C(p^2, k^2, r^2)(\delta_{\mu\nu}p \cdot k - p_\nu k_\mu)(p-k)_\rho \\ & + \frac{1}{3}S(p^2, k^2, r^2)(p_\rho k_\mu r_\nu + p_\nu k_\rho r_\mu) + F(p^2, k^2, r^2)(\delta_{\mu\nu}p \cdot k - p_\nu k_\mu)(p_\rho k \cdot r - k_\rho p \cdot r) \\ & + H(p^2, k^2, r^2) \left[-\delta_{\mu\nu}(p_\rho k \cdot r - k_\rho p \cdot r) + \frac{1}{3}(p_\rho k_\mu r_\nu - p_\nu k_\rho r_\mu) \right] + \text{cyclic permutations} \end{aligned} \quad (4)$$

The scalar functions have the following symmetry properties: A , C and F are symmetric under permutation of the first two arguments; B is antisymmetric under permutation of the first two arguments; H is completely symmetric and S is completely antisymmetric.

It is important to note that only some of these scalar functions are accessible through lattice simulations, since they have access to the vertex function only through the correlation function, i.e. the vertex contracted with the full external propagators. Since the propagators in Lan-

dau gauge are transverse, the longitudinal part of the vertex function is lost in the process. In particular this means that the B and S functions are not accessible through lattice computations.

We decomposed every diagram contributing to the three gluon vertex into the Ball-Chiu tensorial structure. In this way we obtained the contribution of each diagram to each of the scalar functions A, B, C, F, H and S . To perform our computations we expressed the integrals in Feynman diagrams of Fig. 1 in terms of only three Master Integrals defined following the convention on [79] as:

$$\mathbf{A}[m_1] = \bar{C} \int d^d q \frac{1}{[q^2 + m_1^2]} \quad (5)$$

$$\mathbf{B}[p_1, m_1, m_2] = \bar{C} \int d^d q \frac{1}{[q^2 + m_1^2][(q+p_1)^2 + m_2^2]} \quad (6)$$

$$\mathbf{C}[p_1, p_2, m_1, m_2, m_3] = \bar{C} \int d^d q \frac{1}{[q^2 + m_1^2][(q+p_1)^2 + m_2^2][(q-p_2)^2 + m_3^2]} \quad (7)$$

where $\bar{C} = 16\pi^2 \frac{\bar{\mu}^{2\epsilon}}{(2\pi)^d}$, and the regularization scale $\bar{\mu}$ is related to the renormalization scale μ by $\mu^2 = 4\pi e^{-\gamma} \bar{\mu}^2$. The \mathbf{A} and \mathbf{B} - Master Integrals can be solved analytically in $d = 4 - 2\epsilon$ in terms of the external momentum and the masses, but the \mathbf{C} -Master Integral must be treated numerically except for particular kinematics. We chose the FIRE5 algorithm [80] to perform the Master Integral reduction, thus obtaining analytic expressions for each of the scalar functions in terms of the three Master Integrals for arbitrary momentum configurations. The expressions are complicated and not very enlightening, however, the explicit expressions appear in the supplemental material

of [1] for the quenched case while the quark contribution is written in [76]. In the case of one vanishing external momentum the computation becomes much simpler and the result for the quenched vertex function in this configuration is given in [1]¹ while the unquenched case is presented in the Appendix A.

¹ The vanishing momentum configuration in [1] has a misprint, the correct result is shown in the Appendix A

B. Checks

Various checks for the Yang-Mills part of the result for the three-gluon vertex function had already been made in [1]. We only need to check the quark triangle diagram to test our unquenched results. To do this we compared our results to those of [76], verifying that they yield the same expressions when properly transformed to the Euclidean space. This was expected, as the quark triangle diagram is independent from the mass of the gluons and therefore its contribution in the Curci-Ferrari model is the same as in standard QCD.

IV. RENORMALIZATION AND RENORMALIZATION GROUP

In this section we introduce the renormalization scheme that we used in this work and we explain how we implemented renormalization-group ideas to improve our perturbative calculation.

A. Renormalization

To take care of the divergences appearing in the 1-loop quantities we took the usual approach of redefining the fields, masses and coupling constants through renormalization factors that absorb the infinities. The renormalized quantities are defined in terms of the bare ones (denoted with a "0" subscript) as follows:

$$\begin{aligned} A_0^{a\mu} &= \sqrt{Z_A} A^{a\mu}, & \psi_0 &= \sqrt{Z_\psi} \psi, \\ c_0^a &= \sqrt{Z_c} c^a, & \bar{c}_0^a &= \sqrt{Z_c} \bar{c}^a, \\ g_0 &= Z_g g & m_0^2 &= Z_{m^2} m^2 & M_0 &= Z_M M \end{aligned} \quad (8)$$

From now on, all expressions will refer to renormalized quantities unless explicitly stated otherwise. The renormalized propagators and the three-gluon 1PI correlation function are thus defined as:

$$\begin{aligned} \Gamma_{A_\mu^a A_\nu^b}^{(2)}(p) &= Z_A \Gamma_{A_\mu^a A_\nu^b, 0}^{(2)}(p) \\ \Gamma_{c^a \bar{c}^b}^{(2)}(p) &= Z_c \Gamma_{c^a \bar{c}^b, 0}^{(2)}(p) \\ \Gamma_{\psi \bar{\psi}}^{(2)}(p) &= Z_\psi \Gamma_{\psi \bar{\psi}, 0}^{(2)}(p) \\ \Gamma_{A_\mu^a A_\nu^b A_\rho^c}^{(3)}(p, r) &= Z_A^{3/2} \Gamma_{A_\mu^a A_\nu^b A_\rho^c, 0}^{(3)}(p, r) \end{aligned} \quad (9)$$

B. Infrared Safe renormalization scheme

To fix the renormalization factors we used the Infrared Safe (IS) renormalization scheme defined in [42]. It is based on a non-renormalization theorem for the gluon mass [81–83], and is defined by

$$\begin{aligned} \Gamma^\perp(p = \mu) &= m^2 + \mu^2, & J(p = \mu) &= 1, \\ Z_{m^2} Z_A Z_c &= 1. \end{aligned} \quad (10)$$

where $\Gamma^\perp(p)$ is the transversal part of $\Gamma_{A_\mu^a A_\nu^b}^{(2)}(p)$ and $J(p)$ is the ghost dressing function. To fix the renormalization of the coupling constant we used the Taylor scheme, in which the coupling constant is defined as the ghost-gluon vertex with a vanishing ghost momentum. Requiring that the renormalized vertex is finite leads to a relation among the renormalization factors Z_A , Z_c and Z_g :

$$Z_g \sqrt{Z_A} Z_c = 1 \quad (11)$$

The divergent part of the renormalization factors for the quenched case were presented in [42]. Here we show the extension to the unquenched Curci-Ferrari model already computed in [47, 84]. In $d = 4 - 2\epsilon$ they read:

$$\begin{aligned} Z_c &= 1 + \frac{3g^2 N}{64\pi^2 \epsilon} \\ Z_A &= 1 + \frac{g^2}{96\pi^2} \frac{(13N - 8N_f T_f)}{\epsilon} \\ Z_{m^2} &= 1 - \frac{g^2}{192\pi^2} \frac{(35N - 16N_f T_f)}{\epsilon} \\ Z_g &= 1 - \frac{g^2}{96\pi^2} \frac{(11N - 4N_f T_f)}{\epsilon} \end{aligned} \quad (12)$$

Finally, the quantity we are interested in is actually $\Gamma_{\mu\nu\rho}$ as defined earlier. Since in its definition we factorized a factor of g , the relation between the renormalized and bare quantities is the following:

$$\Gamma_{\mu\nu\rho}(p, r) = Z_A^{3/2} Z_g \Gamma_{\mu\nu\rho, 0}(p, r) = \frac{Z_A}{Z_c} \Gamma_{\mu\nu\rho, 0}(p, r),$$

where in the last equality we used equation 11.

C. Renormalization Group

After the renormalization procedure we obtain a finite expression for the three-gluon vertex, but it comes with the usual loop corrections of the form $\log(\frac{\mu}{m_0})$. To handle this situation we implemented the renormalization-group flow to take care of the large logarithms coming from loop corrections. First we define the β functions and anomalous dimensions of the fields:

$$\beta_g(g, m^2) = \mu \frac{dg}{d\mu} \Big|_{g_0, m_0^2}, \quad (13)$$

$$\beta_{m^2}(g, m^2) = \mu \frac{dm^2}{d\mu} \Big|_{g_0, m_0^2}, \quad (14)$$

$$\gamma_A(g, m^2) = \mu \frac{d \log Z_A}{d\mu} \Big|_{g_0, m_0^2}, \quad (15)$$

$$\gamma_c(g, m^2) = \mu \frac{d \log Z_c}{d\mu} \Big|_{g_0, m_0^2}. \quad (16)$$

Analogous expressions are used for the β -function of quark mass and the quark anomalous dimension.

The renormalization group equation for the vertex function with n_A gluon legs and n_c ghost legs reads:

$$\left(\mu \partial_\mu - \frac{1}{2} (n_A \gamma_A + n_c \gamma_c) + \beta_g \partial_g + \beta_{m^2} \partial_{m^2} \right) \Gamma^{(n_A, n_c)} = 0, \quad (17)$$

This equation allows us to obtain a relation for the vertex function renormalized at scale μ_0 and the same vertex function renormalized at a different scale μ :

$$\Gamma^{(n_A, n_c)}(\{p_i\}; \mu, g(\mu), m^2(\mu), M(\mu)) = z_A(\mu)^{n_A/2} z_c(\mu)^{n_c/2} \times \Gamma^{(n_A, n_c)}(\{p_i\}; \mu_0, g(\mu_0), m^2(\mu_0), M(\mu_0)). \quad (18)$$

where $g(\mu)$, $m^2(\mu)$ and $M(\mu)$ are obtained by integration of the β functions with initial conditions given at some scale μ_0 and z_A and z_c are obtained respectively from:

$$\begin{aligned} \log z_A(\mu, \mu_0) &= \int_{\mu_0}^{\mu} \frac{d\mu'}{\mu'} \gamma_A(g(\mu'), m^2(\mu')), \\ \log z_c(\mu, \mu_0) &= \int_{\mu_0}^{\mu} \frac{d\mu'}{\mu'} \gamma_c(g(\mu'), m^2(\mu')). \end{aligned} \quad (19)$$

We can then use the non-renormalization theorems of Eq.(10) and Eq.(11) to relate the anomalous dimensions and the β functions. It is simple to check that one obtains the following relations:

$$\gamma_A(g, m^2) = 2 \left(\frac{\beta_{m^2}}{m^2} - \frac{\beta_g}{g} \right), \quad (20)$$

$$\gamma_c(g, m^2) = \frac{2\beta_g}{g} - \frac{\beta_{m^2}}{m^2}. \quad (21)$$

Finally we use these relations to integrate Eq.(19), obtaining analytical expressions for z_A and z_c in terms of the running gluon mass and coupling constant, being this feature another of the advantages of the Infrared Safe scheme:

$$\begin{aligned} z_A(\mu, \mu_0) &= \frac{m^4(\mu)g^2(\mu_0)}{m^4(\mu_0)g^2(\mu)}, \\ z_c(\mu, \mu_0) &= \frac{m^2(\mu_0)g^2(\mu)}{m^2(\mu)g^2(\mu_0)}. \end{aligned} \quad (22)$$

We are able now to express the three-gluon vertex renormalized at scale μ_0 in terms of the same quantity using a running scale $\mu = p$, thus avoiding the large logarithms problem. Taking into account the factor of g on the definition of $\Gamma_{\mu\nu\rho}(p, r)$ this reads:

$$\Gamma_{\mu\nu\rho}(p, r; \mu_0) = \frac{g^4(p)m^6(\mu_0)}{g^4(\mu_0)m^6(p)} \Gamma_{\mu\nu\rho}(p, r; \mu = p) \quad (23)$$

V. RESULTS

We now present our results for the different scalar functions associated to the three-gluon vertex introduced in the previous section. All our results correspond to four dimensions and the $SU(3)$ gauge group, and we evaluate the scalar functions in different momentum configurations in order to compare them with the available lattice data.

A. Fixing Parameters

The only fitting parameters we need to adjust to compare our results with the lattice are the overall normalization constant of the gluon three-point function and the initial conditions of the renormalization-group flow, i.e. the values of the mass of the gluon, the mass of the quark and the coupling constant at some renormalization scale μ_0 .

The initial conditions for the renormalization-group are best obtained by looking for the set of parameters (m_0 , M_0 , g_0) that produce the best fit between the gluon and ghost propagators computed using the Curci-Ferrari approach and the lattice data, since the lattice results are much more precise for propagators than for three-point functions. This task was done in [1, 50] for different gauge groups and renormalization schemes in the quenched case, and in [47] including dynamical quarks. For the $SU(3)$ group and the IS scheme the initial conditions for the R-G flow at $\mu_0 = 1$ GeV obtained are the ones listed in table I .

	m_0 (GeV)	M_0 (GeV)	g_0
Quenched	0.35	-	3.6
Unquenched ($N_f = 2$)	0.42	0.13	4.5

TABLE I. Values of the masses of the quark and gluon (M_0 and m_0 respectively) and the coupling constant (g_0) at renormalization scale $\mu_0 = 1$ GeV obtained by adjusting the 2-point functions to lattice data, both for the quenched case and the unquenched case with two degenerate quark flavors.

In this work we use these values to compute the one loop three-gluon vertex, which means that up to the overall normalization constant our results are a pure prediction of the model.

B. Comparison with the lattice

In order to compare with the lattice, we must choose specific momentum configurations for $\Gamma_{\mu\nu\rho}(p_1, p_2, p_3)$. Most available lattice data employs some of the following configurations: The *Symmetric Configuration*, with $p_1^2 = p_2^2 = p_3^2 = p^2$ and $p_1 \cdot p_2 = p_1 \cdot p_3 = p_2 \cdot p_3 = -\frac{p^2}{2}$, the *Asymmetric Configuration*, with $p_1 = 0$ and

$p_2 = -p_3 = p$, and the *Orthogonal Configuration*, with $p_1 \cdot p_2 = 0$, $p_1^2 = p_2^2 = p^2$ and $p_3^2 = 2p^2$.

For the quenched case, we compared our results with the lattice data from [2]. Following their definitions, in the symmetric configuration we work with the scalar functions $\bar{\Gamma}_1^{\text{sym}}$ and $\bar{\Gamma}_2^{\text{sym}}$:

$$g\Gamma_{\mu\nu\rho}(p_1, p_2, p_3) = \bar{\Gamma}_1^{\text{sym}}(s^2) \lambda_1^{\mu\nu\rho}(p_1, p_2, p_3) + \bar{\Gamma}_2^{\text{sym}}(s^2) \lambda_2^{\mu\nu\rho}(p_1, p_2, p_3), \quad (24)$$

where

$$\lambda_1^{\mu\nu\rho}(p_1, p_2, p_3) = \Gamma_{\mu'\nu'\rho'}^{(0)}(p_1, p_2, p_3) P_{\mu'\mu}^\perp(p_1) P_{\nu'\nu}^\perp(p_2) P_{\rho'\rho}^\perp(p_3),$$

with $\Gamma_{\mu'\nu'\rho'}^{(0)}(p_1, p_2, p_3)$ defined as the perturbative tree-level tensor of the three-gluon vertex, and

$$G_1(p, k, r) = \frac{[(r-k)_\gamma \delta_{\alpha\beta} + \text{cyclic permutations}] P_{\alpha\mu}^\perp(p) P_{\beta\nu}^\perp(k) P_{\gamma\rho}^\perp(r) \Gamma_{\mu\nu\rho}(p, k, r)}{[(r-k)_\gamma \delta_{\alpha\beta} + \text{cyclic permutations}] P_{\alpha\mu}^\perp(p) P_{\beta\nu}^\perp(k) P_{\gamma\rho}^\perp(r) [(r-k)_\rho \delta_{\mu\nu} + \text{cyclic permutations}]} \quad (27)$$

The results of the model are shown below using the different scalar functions defined in this section including the renormalization group effects.

C. $SU(3)$ Yang Mills results

We first present our results for $SU(3)$ Yang Mills theory and we compare them with lattice results from [2]. As stated before, we integrate the beta functions with initial conditions at $\mu_0 = 1$ GeV using the initial conditions listed in table I.

In Fig. 2 we show the results for the scalar function $\bar{\Gamma}_3^{\text{asym}}$ in the asymmetric configuration (one vanishing momentum), and in Fig. 3 we do the same for the functions $\bar{\Gamma}_1^{\text{sym}}$ and $\bar{\Gamma}_2^{\text{sym}}$ the symmetric configuration (all momenta equal).

In all cases the agreement is very good, specially considering that the initial conditions for the renormalization-group flow were not fitted for the three-point function but for the propagators. It is also noticeable that in all cases the different scalar functions become negative at low energies, a qualitative feature that was observed in many lattice simulations as well as in different analysis [56, 62, 65–68]. While the scalar functions associated to the tree-level tensor diverges logarithmically the $\bar{\Gamma}_2^{\text{sym}}$ goes to a constant value in the infrared as stated in [2]. The simplicity of one-loop CF model allows to write the infrared behaviour of $\bar{\Gamma}_2^{\text{sym}}$ analytically:

$$\lambda_2^{\mu\nu\rho}(p_1, p_2, p_3) = \frac{(p_1 - p_2)_\rho (p_2 - p_3)_\mu (p_3 - p_1)_\nu}{p^2}.$$

On the other hand the asymmetric configuration of the vertex is parametrized by a single scalar function $\bar{\Gamma}_3^{\text{asym}}$ defined by

$$g\Gamma_{\mu\nu\rho}(p, -p, 0) = \bar{\Gamma}_3^{\text{asym}}(p^2) \lambda_3^{\mu\nu\rho}(p, -p, 0), \quad (25)$$

with

$$\lambda_3^{\mu\nu\rho}(p, -p, 0) = 2p^\rho P^{\perp\mu\nu}(p). \quad (26)$$

We compared our unquenched results with the lattice data from [70]. They work in the orthogonal configuration, and define the usual scalar function G_1 , which consists on contracting the external legs of the vertex with transverse propagators and the tree-level momentum structure of the 3-gluon vertex, normalized to the same expression at tree-level. This reads:

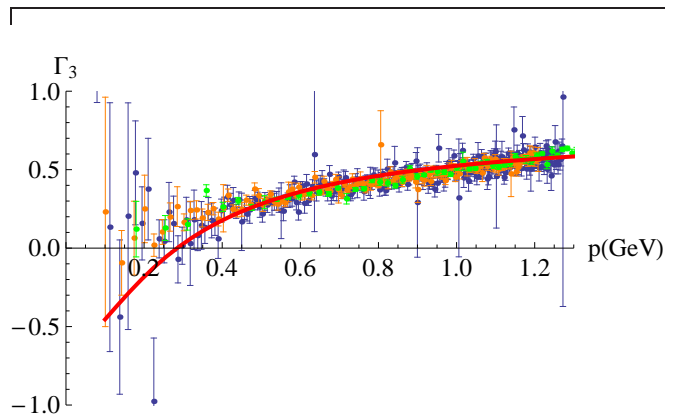


FIG. 2. $\bar{\Gamma}_3^{\text{asym}}$ scalar function as a function of momentum for one vanishing momentum (asymmetric configuration). The points are lattice data from [2]. The plain red line corresponds to our 1-loop computation.

$$\bar{\Gamma}_2^{\text{sym}} \sim \frac{g^2 N}{414720\pi^2} \left(20 \left(16\sqrt{3} \text{Cl}_2 \left(\frac{\pi}{3} \right) - 33 \right) + 189 \frac{p^2}{m^2} \right) \quad (28)$$

where Cl_2 is the Clausen function and $\text{Cl}_2 \left(\frac{\pi}{3} \right) = 1.0149417$. We observe that the analytical expression indicates that the $\bar{\Gamma}_2^{\text{sym}}$ goes to a constant value in the infrared and this situation is not modified with the effects of the renormalization group.

These expressions show the divergent behavior for $\bar{\Gamma}_1$, that can be easily understood due to the presence of

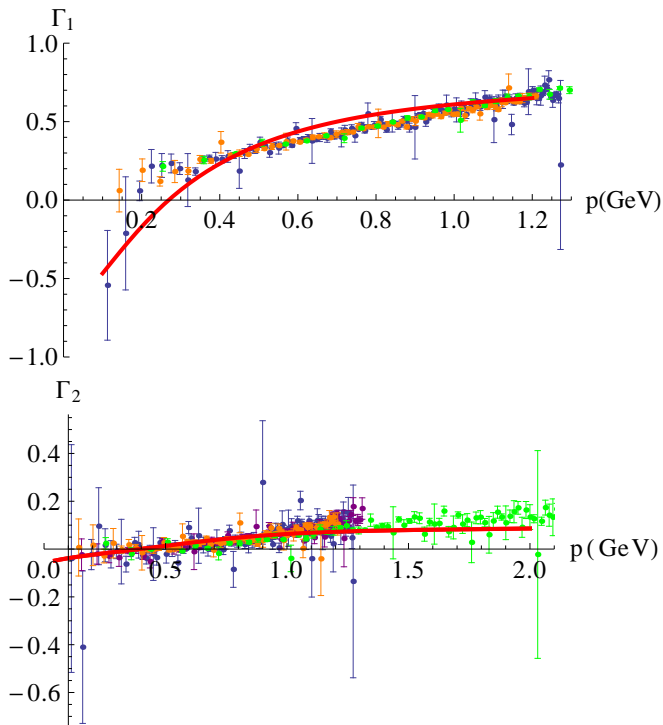


FIG. 3. $\bar{\Gamma}_1^{\text{sym}}$ (top) and $\bar{\Gamma}_2^{\text{sym}}$ (bottom) scalar functions as a function of momentum for all momenta equal (symmetric configuration). The points are lattice data from [2]. The plain red line corresponds to our 1-loop computation.

massless ghosts as stated in [1]. As observed in [2], it is also found that $\bar{\Gamma}_2^{\text{sym}}$ is finite in the infrared.

D. Unquenched QCD results

If we want to include the influence of dynamical quarks to the previous computation we must add only the triangle diagram with a loop of quarks to the vertex but also include the running of the coupling obtained in the unquenched analysis [47]. The contribution of that diagram can be computed with no difficulty in arbitrary dimension and for arbitrary number of quarks. Our explicit expressions match with the ones presented in [76] when transforming to Euclidean space. In order to be more specific we show as an example the explicit bare contribution of the quark-loop diagram to the factor G_1 in $d = 4 - 2\epsilon$ dimensions in Appendix B. In Fig. 4 we show the results and their comparison with lattice data from [70]. The data available corresponds to the G_1 scalar function in the case of two mass-degenerate quark flavors ($N_f = 2$) in the orthogonal configuration (two momenta orthogonal to each other and of equal magnitude).

In this case, the agreement is still very good in the infrared but worsens in the UV. More precisely, the model and the lattice results start separating at a scale of about 2.5 GeV. This scale is of the order of magnitude of the inverse of the lattice spacing used in most lattice sim-

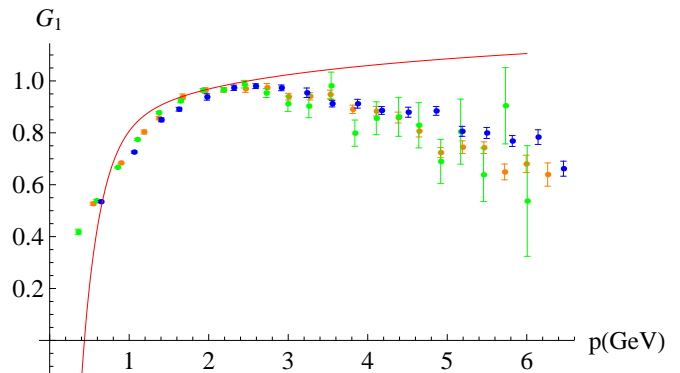


FIG. 4. G_1 scalar function as a function of momentum for two momenta orthogonal (orthogonal configuration) and two mass-degenerate quark flavors. The points are lattice data from [70]. The plain red line corresponds to our 1-loop computation.

ulations, and therefore lattice results beyond this scale are subject to hypercubic lattice spacing artefacts. Taking this fact into account and also considering that perturbation theory must work at one-loop in the UV, we suspected that the decrease in the values of G_1 after the inverse lattice spacing scale must be caused by finite lattice artefacts such as lattice effects in the UV.

To confirm this statement, we computed analytically the high-energy limit of G_1 , finding that it behaves in the UV as $\text{Ln}(\frac{p}{\mu_0})^\alpha$ with $\alpha = \frac{17N - 16N_f T_f}{44N - 16N_f T_f}$, which is compatible with our results. The idea behind this computation is that since the UV limit of $G_1(p, p)$ is equal to 1, the high-energy behavior of $G_1(\mu_0, p)$ must be given by $z_A^{-\frac{3}{2}}$ as a consequence of the renormalization-group equation given in Eq. (17). The full computation shows that the UV limit of $z_A^{-\frac{3}{2}}$ is indeed $z_A^{-\frac{3}{2}} \propto \text{Ln}(\frac{\mu}{\mu_0})^{\frac{35}{116}}$ for $N = 3$ and $N_f = 2$. In conclusion, our one-loop computation matches the lattice results in their regime of validity and the renormalization-group prediction in the UV.

1. Zero crossing and the number of flavours.

In this section we study the influence of dynamical quarks in the position of the zero crossing of the three-gluon vertex. In the one-loop CF-model the influence of quarks in the renormalized vertex can be isolated as the term proportional to N_f . At one loop, the quarks contribution to the renormalized vertex is proportional to:

$$\mathcal{F} = \left(\frac{3}{2} \delta Z_A^{UQ} \Big|_{finite} + G_1^{UQ} \Big|_{finite} \right)$$

where $\delta Z_A^{UQ} \Big|_{finite}$ and $G_1^{UQ} \Big|_{finite}$ represent the finite part of the coefficient proportional to $g^2 N_f T_f$ in the Z_A -

renormalization factor and in G_1 respectively.

We study here the sign of the factor, \mathcal{F} , in order to analyze in which direction the zero crossing is shifted. As \mathcal{F} depends on the finite part of the renormalization factor, it is expected that its sign depends on the chosen renormalization scheme. Moreover, we also observe that it depends on the kinematical configuration of the vertex function. In order to do analyze this fact we simplify the expression by taking two momenta of equal norm and study the behavior of the factor \mathcal{F} at low momentum as a function of the angle between the chosen momenta.

The dependence \mathcal{F} on the renormalization scheme of can be observed in Fig. 5 where \mathcal{F} is depicted in the case when no contribution for the finite part of the renormalization factor is taken into account and when \mathcal{F} is evaluated in the IS-scheme. The plot is done by setting $\bar{\mu} = 1$ GeV for the regularization scale, $M = 0.36$ GeV for the value of the constituent quark's mass and for momentum $p = 0.27$ GeV, as this is approximately the value of the momentum at which the zero crossing is observed. This shows that different renormalization schemes can indeed yield directions for the shift of the zero crossing caused by the quarks contribution to the vertex.

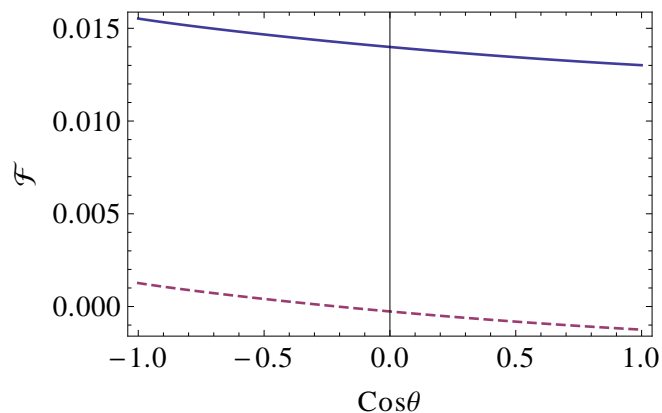


FIG. 5. \mathcal{F} at $\bar{\mu} = 1$ GeV, $M = 0.36$ GeV and $p = 0.27$ GeV in the case of $\delta Z_A^{UQ} \Big|_{finite} = 0$ (upper) and in the IS-scheme (lower) as a function of $\text{Cos}(\theta)$ (the cosine of the angle between the two chosen momenta)

Focusing now on the IS-scheme only, we analyzed the dependence of the factor \mathcal{F} on the kinematical configuration for two particular values of the momentum $p = 0.2$ GeV and 0.27 GeV in Fig. 6. These values were chosen taken into account the observation that the zero crossing occurs for values of p below 0.3 We considered quark masses in the region between $0.3 - 0.36$ GeV which correspond to the infrared values. For completeness we also studied in Fig. 7 the sign of \mathcal{F} as a function of the quark mass for the antisymmetric ($\text{Cos}(\theta) = -1$), symmetric ($\text{Cos}(\theta) = -1/2$), orthogonal ($\text{Cos}(\theta) = 0$) and parallel ($\text{Cos}(\theta) = 1$) kinematical configurations, where it is shown again that the position of the zero crossing changes with the presence of dynamical quarks but the

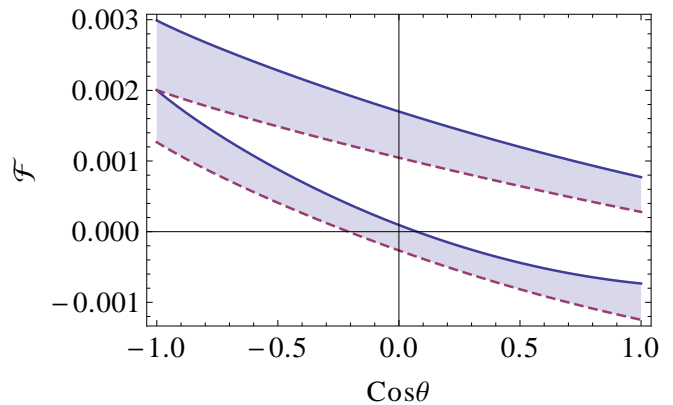


FIG. 6. \mathcal{F} as a function of $\text{Cos}(\theta)$ computed in the IS-scheme. Regions represent different values of M between $0.3 - 0.36$ GeV, while the upper region is for $p = 0.2$ GeV and the lower region corresponds to $p = 0.27$ GeV.

direction depends on the kinematical configuration.

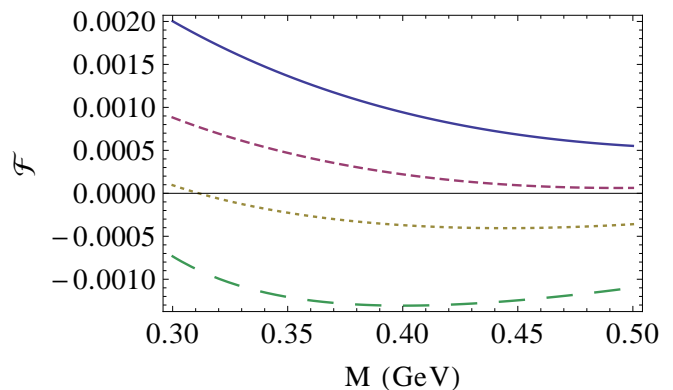


FIG. 7. Plots correspond to the IS- \mathcal{F} factor as a function of the quark mass evaluated in $p = 0.27$ GeV for different kinematical configurations, from top to bottom: the antisymmetric ($\text{Cos}(\theta) = -1$), symmetric ($\text{Cos}(\theta) = -1/2$), orthogonal ($\text{Cos}(\theta) = 0$) and parallel ($\text{Cos}(\theta) = 1$) kinematical configurations.

It is worth noting from Fig. 7 that dynamical quarks move the zero crossing towards the infrared in the symmetric configuration (as observed in [60]) while it is shifted in the opposite direction in the orthogonal configuration. Fig. 8 shows the study of the orthogonal case in detail when including the effects of the renormalization group. It can be seen that the zero crossing is moved towards the ultraviolet when including dynamical quarks as expected from the previous analysis. We conclude from this analysis that the position of the zero crossing is shifted with the presence of quarks but the direction of the shift depends on the kinematical configuration and on the renormalization scheme where the vertex is analyzed.

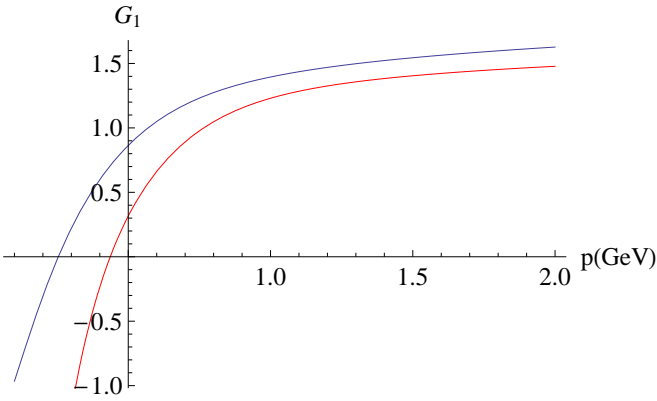


FIG. 8. G_1 scalar function as a function p for in the orthogonal configuration for $N_f = 0$ (blue) and $N_f = 2$ (red). The position of the zero crossing is shifted towards the UV by the quark's contribution in this configuration.

VI. CONCLUSIONS

With the aim of studying the infrared properties of the three-point correlation function, in this article, we present a one-loop calculation using Curci-Ferrari model in Landau gauge for arbitrary kinematical configuration. The results are an extension of a previous work [1] to the unquenched case. In particular, we compare the results for the vertex with the available lattice data including dynamical quarks that corresponds to the kinematical configuration with a vanishing gluon momentum and two degenerate flavors. A study of the position of the zero crossing as a function of the kinematical configuration of the vertex is done. It is observed that the position of the zero crossing is shifted due to the presence of dynamical quarks when comparing with the quenched case.

However, the direction of the shift depends on the chosen renormalization scheme and on the kinematical configuration of the vertex.

We also study the quenched case because some infrared properties observed by the model in the previous work were not clear in lattice simulations at that time. However, the infrared lattice study of the three-gluon vertex has improved in the last years and now error bars are good enough to understand its infrared behavior as discussed in [2]. In particular, lattice simulations show a change of sign in the deep infrared that is easily understood by Curci-Ferrari model. As it has been discussed in [1, 56] it can be explained as a consequence of the diagram with a loop of massless ghosts. In the quenched case we compare the results with lattice simulations for the completely symmetric and the antisymmetric configuration. The results are really good, specially considering that the free parameters of the model were already fixed by fitting the propagators.

ACKNOWLEDGMENTS

The authors would like to acknowledge the financial support from PEDECIBA and ECOS program and from the ANII-FCE-126412 project. We also thank N. Barrios, U. Reinoso, M. Tissier and N. Wschebor for useful discussions.

Appendix A: One-loop three-gluon vertex in the vanishing momentum configuration

We correct in this Appendix a misprint in the result of the one-loop three-gluon vertex expression in the vanishing momentum configuration.

$$\begin{aligned}
\Gamma_{\mu\nu\rho}(0, p, -p) = & \left\{ 1 - \frac{Ng_0^2}{768\pi^2} \left[\frac{136}{2\epsilon}(1 - 2\epsilon \log \bar{m}) + \frac{1}{3}(36s^{-2} - 594s^{-1} + 319 + 6s) + (3s^2 - 2) \log s \right. \right. \\
& - 4s^{-3}(1+s)^3(s^2 - 9s + 3) \log(1+s) \\
& \left. \left. + \frac{(4+s)^{3/2}}{s^{3/2}} (24 - 30s + s^2) \log \left(\frac{\sqrt{4+s} + \sqrt{s}}{\sqrt{4+s} - \sqrt{s}} \right) \right] \right\} (p_\nu \delta_{\mu\rho} + p_\rho \delta_{\nu\mu}) \\
& - \left\{ 2 + \frac{Ng_0^2}{384\pi^2} \left[-\frac{136}{2\epsilon}(1 - 2\epsilon \log \bar{m}) + \frac{1}{3}(18s^{-2} - 321s^{-1} - 97 + 24s) + (s-1)(s^2 - 2s - 2) \log s \right. \right. \\
& - 2s^{-3}(1+s)^2(s-1)(s^3 - 7s^2 + 7s - 3) \log(1+s) \\
& \left. \left. + \frac{\sqrt{4+s}}{s^{3/2}} (48 + 16s + 22s^2 - 11s^3 + s^4) \log \left(\frac{\sqrt{4+s} + \sqrt{s}}{\sqrt{4+s} - \sqrt{s}} \right) \right] \right\} p_\mu \delta_{\nu\rho} \\
& - \frac{Ng_0^2}{384\pi^2 m^2} \left[(-36s^{-3} + 278s^{-2} - 74s^{-1} - 10) - s^2 \log s \right. \\
& \left. + s^{-3}(1+s)^2(36s^{-1} - 44 - 4s - 12s^2 + 2s^3) \log(1+s) \right. \\
& \left. + \sqrt{s(4+s)} s^{-3} (-144s^{-1} + 80 + 4s + 10s^2 - s^3) \log \left(\frac{\sqrt{4+s} + \sqrt{s}}{\sqrt{4+s} - \sqrt{s}} \right) \right] p_\nu p_\mu p_\rho
\end{aligned} \tag{A1}$$

where $s = \frac{p^2}{m^2}$ and $\bar{m}^2 = m^2 e^\gamma / (4\pi)$, with γ the Euler constant.

Appendix B: Contribution of dynamical quarks

The contribution of dynamical quarks to the G_1 factor:

$$\begin{aligned} & \frac{g^2 N_f T_f}{12\pi^2 \epsilon} + \frac{g^2 N_f T_f}{12\pi^2} \left[-\frac{1}{3} + \frac{2\chi (A_0 (M^2) + M^2)}{D_1} + \frac{1}{D_1 D_2} \left(24k^2 p^2 r^2 C_0 (M^2, M^2, M^2, p, r) (\mathcal{S} - M^2 \chi) \right. \right. \\ & \left. \left. + \mathcal{K}_1 B_0 (M^2, M^2, -p^2) + \mathcal{K}_2 B_0 (M^2, M^2, -r^2) + \mathcal{K}_3 B_0 (M^2, M^2, -k^2) \right) \right] \end{aligned} \quad (\text{B1})$$

where A_0 , B_0 and C_0 are the corresponding finite part of master integrals defined in Eq. ?? and

$$\begin{aligned} \chi &= p^2 + r^2 + k^2, \\ \mathcal{S} &= p^2 r^2 + p^2 k^2 + r^2 k^2, \\ D_1 &= k^4 + p^4 + r^4 + 10\mathcal{S}, \\ D_2 &= k^4 + p^4 + r^4 - 2\mathcal{S} \end{aligned}$$

and

$$\begin{aligned} \mathcal{K}_1 &= k^6 (2M^2 - p^2) + k^4 (2M^2 (9p^2 - r^2) - 9p^4 - 11p^2 r^2) \\ & - k^2 (2M^2 (9p^4 + 2p^2 r^2 + r^4) - 9p^6 + 10p^4 r^2 + 11p^2 r^4) \\ & - (2M^2 - p^2) (p^6 + 9p^4 r^2 - 9p^2 r^4 - r^6) \end{aligned}$$

while \mathcal{K}_2 and \mathcal{K}_3 are obtained exchanging $p \leftrightarrow r$ and $p \leftrightarrow k$ in \mathcal{K}_1 respectively.

-
- [1] M. Pelaez, M. Tissier and N. Wschebor, Phys. Rev. D **88** (2013), 125003 doi:10.1103/PhysRevD.88.125003 [arXiv:1310.2594 [hep-th]].
- [2] A. C. Aguilar, F. De Soto, M. N. Ferreira, J. Papavassiliou and J. Rodríguez-Quintero, Phys. Lett. B **818** (2021), 136352 doi:10.1016/j.physletb.2021.136352 [arXiv:2102.04959 [hep-ph]].
- [3] R. Alkofer and L. von Smekal, Phys. Rept. **353** (2001), 281 doi:10.1016/S0370-1573(01)00010-2 [arXiv:hep-ph/0007355 [hep-ph]].
- [4] L. von Smekal, R. Alkofer and A. Hauck, Phys. Rev. Lett. **79** (1997), 3591-3594 doi:10.1103/PhysRevLett.79.3591 [arXiv:hep-ph/9705242 [hep-ph]].
- [5] D. Atkinson and J. C. R. Bloch, Mod. Phys. Lett. A **13** (1998), 1055-1062 doi:10.1142/S0217732398001121 [arXiv:hep-ph/9802239 [hep-ph]].
- [6] D. Zwanziger, Phys. Rev. D **65** (2002), 094039 doi:10.1103/PhysRevD.65.094039 [arXiv:hep-th/0109224 [hep-th]].
- [7] C. Lerche and L. von Smekal, Phys. Rev. D **65** (2002), 125006 doi:10.1103/PhysRevD.65.125006 [arXiv:hep-ph/0202194 [hep-ph]].
- [8] C. S. Fischer and R. Alkofer, Phys. Lett. B **536** (2002), 177-184 doi:10.1016/S0370-2693(02)01809-9 [arXiv:hep-ph/0202202 [hep-ph]].
- [9] A. Maas, J. Wambach, B. Gruter and R. Alkofer, Eur. Phys. J. C **37** (2004), 335-357 doi:10.1140/epjc/s2004-02004-3 [arXiv:hep-ph/0408074 [hep-ph]].
- [10] P. Boucaud, T. Bruntjen, J. P. Leroy, A. Le Yaouanc, A. Y. Lokhov, J. Micheli, O. Pene and J. Rodríguez-Quintero, JHEP **06** (2006), 001 doi:10.1088/1126-6708/2006/06/001 [arXiv:hep-ph/0604056 [hep-ph]].
- [11] M. Q. Huber, R. Alkofer, C. S. Fischer and K. Schwenzer, Phys. Lett. B **659** (2008), 434-440 doi:10.1016/j.physletb.2007.10.073 [arXiv:0705.3809 [hep-ph]].
- [12] A. C. Aguilar and J. Papavassiliou, J. Phys. Conf. Ser. **110** (2008), 022040 doi:10.1088/1742-6596/110/2/022040 [arXiv:0711.0936 [hep-ph]].
- [13] A. C. Aguilar, D. Binosi and J. Papavassiliou, Phys. Rev. D **78** (2008), 025010 doi:10.1103/PhysRevD.78.025010 [arXiv:0802.1870 [hep-ph]].
- [14] P. Boucaud, J. P. Leroy, A. L. Yaouanc, J. Micheli, O. Pene and J. Rodríguez-Quintero, JHEP **06** (2008), 012 doi:10.1088/1126-6708/2008/06/012 [arXiv:0801.2721 [hep-ph]].
- [15] P. Dall'Olivo, J. Phys. Conf. Ser. **378** (2012), 012037 doi:10.1088/1742-6596/378/1/012037
- [16] M. Q. Huber, A. Maas and L. von Smekal, JHEP **11** (2012), 035 doi:10.1007/JHEP11(2012)035 [arXiv:1207.0222 [hep-th]].
- [17] M. Q. Huber, Phys. Rev. D **93** (2016) no.8, 085033

- doi:10.1103/PhysRevD.93.085033 [arXiv:1602.02038 [hep-th]].
- [18] M. Q. Huber, *Phys. Rev. D* **101** (2020), 114009 doi:10.1103/PhysRevD.101.114009 [arXiv:2003.13703 [hep-ph]].
- [19] U. Ellwanger, M. Hirsch and A. Weber, *Eur. Phys. J. C* **1** (1998), 563-578 doi:10.1007/s100520050105 [arXiv:hep-ph/9606468 [hep-ph]].
- [20] J. M. Pawłowski, D. F. Litim, S. Nedelko and L. von Smekal, *Phys. Rev. Lett.* **93** (2004), 152002 doi:10.1103/PhysRevLett.93.152002 [arXiv:hep-th/0312324 [hep-th]].
- [21] C. S. Fischer and H. Gies, *JHEP* **10** (2004), 048 doi:10.1088/1126-6708/2004/10/048 [arXiv:hep-ph/0408089 [hep-ph]].
- [22] C. S. Fischer and J. M. Pawłowski, *Phys. Rev. D* **75** (2007), 025012 doi:10.1103/PhysRevD.75.025012 [arXiv:hep-th/0609009 [hep-th]].
- [23] C. S. Fischer, A. Maas and J. M. Pawłowski, *Annals Phys.* **324** (2009), 2408-2437 doi:10.1016/j.aop.2009.07.009 [arXiv:0810.1987 [hep-ph]].
- [24] A. K. Cyrol, L. Fister, M. Mitter, J. M. Pawłowski and N. Strodthoff, *Phys. Rev. D* **94** (2016) no.5, 054005 doi:10.1103/PhysRevD.94.054005 [arXiv:1605.01856 [hep-ph]].
- [25] N. Dupuis, L. Canet, A. Eichhorn, W. Metzner, J. M. Pawłowski, M. Tissier and N. Wschebor, *Phys. Rept.* **910** (2021), 1-114 doi:10.1016/j.physrep.2021.01.001 [arXiv:2006.04853 [cond-mat.stat-mech]].
- [26] V. N. Gribov, *Nucl. Phys. B* **139** (1978), 1 doi:10.1016/0550-3213(78)90175-X
- [27] D. Zwanziger, *Nucl. Phys. B* **323** (1989), 513-544 doi:10.1016/0550-3213(89)90122-3
- [28] N. Vandersickel and D. Zwanziger, *Phys. Rept.* **520** (2012), 175-251 doi:10.1016/j.physrep.2012.07.003 [arXiv:1202.1491 [hep-th]].
- [29] D. Dudal, J. A. Gracey, S. P. Sorella, N. Vandersickel and H. Verschelde, *Phys. Rev. D* **78** (2008), 065047 doi:10.1103/PhysRevD.78.065047 [arXiv:0806.4348 [hep-th]].
- [30] F. D. R. Bonnet, P. O. Bowman, D. B. Leinweber and A. G. Williams, *Phys. Rev. D* **62** (2000), 051501 doi:10.1103/PhysRevD.62.051501 [arXiv:hep-lat/0002020 [hep-lat]].
- [31] F. D. R. Bonnet, P. O. Bowman, D. B. Leinweber, A. G. Williams and J. M. Zanotti, *Phys. Rev. D* **64** (2001), 034501 doi:10.1103/PhysRevD.64.034501 [arXiv:hep-lat/0101013 [hep-lat]].
- [32] A. Cucchieri and T. Mendes, *Phys. Rev. Lett.* **100** (2008), 241601 doi:10.1103/PhysRevLett.100.241601 [arXiv:0712.3517 [hep-lat]].
- [33] I. L. Bogolubsky, E. M. Ilgenfritz, M. Müller-Preussker and A. Sternbeck, *Phys. Lett. B* **676** (2009), 69-73 doi:10.1016/j.physletb.2009.04.076 [arXiv:0901.0736 [hep-lat]].
- [34] V. G. Bornyakov, V. K. Mitryushkin and M. Müller-Preussker, *Phys. Rev. D* **81** (2010), 054503 doi:10.1103/PhysRevD.81.054503 [arXiv:0912.4475 [hep-lat]].
- [35] T. Iritani, H. Suganuma and H. Iida, *Phys. Rev. D* **80** (2009), 114505 doi:10.1103/PhysRevD.80.114505 [arXiv:0908.1311 [hep-lat]].
- [36] A. Maas, *Phys. Rept.* **524** (2013), 203-300 doi:10.1016/j.physrep.2012.11.002 [arXiv:1106.3942 [hep-ph]].
- [37] O. Oliveira and P. J. Silva, *Phys. Rev. D* **86** (2012), 114513 doi:10.1103/PhysRevD.86.114513 [arXiv:1207.3029 [hep-lat]].
- [38] P. Boucaud, J. P. Leroy, A. L. Yaouanc, J. Micheli, O. Pene and J. Rodríguez-Quintero, *Few Body Syst.* **53** (2012), 387-436 doi:10.1007/s00601-011-0301-2 [arXiv:1109.1936 [hep-ph]].
- [39] P. Boucaud, F. De Soto, K. Raya, J. Rodríguez-Quintero and S. Zafeiropoulos, *Phys. Rev. D* **98**, no.11, 114515 (2018) doi:10.1103/PhysRevD.98.114515 [arXiv:1809.05776 [hep-ph]].
- [40] S. Zafeiropoulos, P. Boucaud, F. De Soto, J. Rodríguez-Quintero and J. Segovia, *Phys. Rev. Lett.* **122**, no.16, 162002 (2019) doi:10.1103/PhysRevLett.122.162002 [arXiv:1902.08148 [hep-ph]].
- [41] M. Tissier and N. Wschebor, *Phys. Rev. D* **82** (2010), 101701 doi:10.1103/PhysRevD.82.101701 [arXiv:1004.1607 [hep-ph]].
- [42] M. Tissier and N. Wschebor, *Phys. Rev. D* **84** (2011), 045018 doi:10.1103/PhysRevD.84.045018 [arXiv:1105.2475 [hep-th]].
- [43] G. Curci and R. Ferrari, *Nuovo Cim. A* **32** (1976), 151-168 doi:10.1007/BF02729999
- [44] M. Peláez, U. Reinosa, J. Serreau, M. Tissier and N. Wschebor, *Phys. Rev. D* **96**, no.11, 114011 (2017) doi:10.1103/PhysRevD.96.114011 [arXiv:1703.10288 [hep-th]].
- [45] M. Peláez, U. Reinosa, J. Serreau, M. Tissier and N. Wschebor, *Phys. Rev. D* **103**, no.9, 094035 (2021) doi:10.1103/PhysRevD.103.094035 [arXiv:2010.13689 [hep-ph]].
- [46] M. Peláez, U. Reinosa, J. Serreau, M. Tissier and N. Wschebor, [arXiv:2106.04526 [hep-th]].
- [47] M. Peláez, M. Tissier and N. Wschebor, *Phys. Rev. D* **90** (2014), 065031 doi:10.1103/PhysRevD.90.065031 [arXiv:1407.2005 [hep-th]].
- [48] M. Peláez, M. Tissier and N. Wschebor, *Phys. Rev. D* **92** (2015) no.4, 045012 doi:10.1103/PhysRevD.92.045012 [arXiv:1504.05157 [hep-th]].
- [49] U. Reinosa, J. Serreau, M. Tissier and N. Wschebor, *Phys. Rev. D* **96** (2017) no.1, 014005 doi:10.1103/PhysRevD.96.014005 [arXiv:1703.04041 [hep-th]].
- [50] J. A. Gracey, M. Peláez, U. Reinosa and M. Tissier, *Phys. Rev. D* **100** (2019) no.3, 034023 doi:10.1103/PhysRevD.100.034023 [arXiv:1905.07262 [hep-th]].
- [51] N. Barrios, J. A. Gracey, M. Peláez and U. Reinosa, [arXiv:2103.16218 [hep-th]].
- [52] N. Barrios, M. Peláez, U. Reinosa and N. Wschebor, *Phys. Rev. D* **102** (2020), 114016 doi:10.1103/PhysRevD.102.114016 [arXiv:2009.00875 [hep-th]].
- [53] R. Alkofer, C. S. Fischer and F. J. Llanes-Estrada, *Phys. Lett. B* **611** (2005), 279-288 [erratum: *Phys. Lett. B* **670** (2009), 460-461] doi:10.1016/j.physletb.2008.11.068 [arXiv:hep-th/0412330 [hep-th]].
- [54] A. Cucchieri, A. Maas and T. Mendes, *Phys. Rev. D* **74** (2006), 014503 doi:10.1103/PhysRevD.74.014503 [arXiv:hep-lat/0605011 [hep-lat]].
- [55] A. Cucchieri, A. Maas and T. Mendes, *Phys. Rev.*

- D **77** (2008), 094510 doi:10.1103/PhysRevD.77.094510 [arXiv:0803.1798 [hep-lat]].
- [56] A. C. Aguilar, D. Binosi, D. Ibañez and J. Papavassiliou, Phys. Rev. D **89** (2014) no.8, 085008 doi:10.1103/PhysRevD.89.085008 [arXiv:1312.1212 [hep-ph]].
- [57] A. Blum, M. Q. Huber, M. Mitter and L. von Smekal, Phys. Rev. D **89** (2014), 061703 doi:10.1103/PhysRevD.89.061703 [arXiv:1401.0713 [hep-ph]].
- [58] G. Eichmann, R. Williams, R. Alkofer and M. Vujanovic, Phys. Rev. D **89** (2014) no.10, 105014 doi:10.1103/PhysRevD.89.105014 [arXiv:1402.1365 [hep-ph]].
- [59] M. Mitter, J. M. Pawłowski and N. Strodthoff, Phys. Rev. D **91** (2015), 054035 doi:10.1103/PhysRevD.91.054035 [arXiv:1411.7978 [hep-ph]].
- [60] R. Williams, C. S. Fischer and W. Heupel, Phys. Rev. D **93** (2016) no.3, 034026 doi:10.1103/PhysRevD.93.034026 [arXiv:1512.00455 [hep-ph]].
- [61] A. L. Blum, R. Alkofer, M. Q. Huber and A. Windisch, Acta Phys. Polon. Supp. **8** (2015) no.2, 321 doi:10.5506/APhysPolBSupp.8.321 [arXiv:1506.04275 [hep-ph]].
- [62] A. Athenodorou, D. Binosi, P. Boucaud, F. De Soto, J. Papavassiliou, J. Rodríguez-Quintero and S. Zafeiropoulos, Phys. Lett. B **761** (2016), 444-449 doi:10.1016/j.physletb.2016.08.065 [arXiv:1607.01278 [hep-ph]].
- [63] A. G. Duarte, O. Oliveira and P. J. Silva, Phys. Rev. D **94** (2016) no.7, 074502 doi:10.1103/PhysRevD.94.074502 [arXiv:1607.03831 [hep-lat]].
- [64] L. Corell, A. K. Cyrol, M. Mitter, J. M. Pawłowski and N. Strodthoff, SciPost Phys. **5** (2018) no.6, 066 doi:10.21468/SciPostPhys.5.6.066 [arXiv:1803.10092 [hep-ph]].
- [65] P. Boucaud, F. De Soto, J. Rodríguez-Quintero and S. Zafeiropoulos, Phys. Rev. D **95** (2017) no.11, 114503 doi:10.1103/PhysRevD.95.114503 [arXiv:1701.07390 [hep-lat]].
- [66] A. C. Aguilar, M. N. Ferreira, C. T. Figueiredo and J. Papavassiliou, Phys. Rev. D **99** (2019) no.9, 094010 doi:10.1103/PhysRevD.99.094010 [arXiv:1903.01184 [hep-ph]].
- [67] A. C. Aguilar, F. De Soto, M. N. Ferreira, J. Papavassiliou, J. Rodríguez-Quintero and S. Zafeiropoulos, Eur. Phys. J. C **80** (2020) no.2, 154 doi:10.1140/epjc/s10052-020-7741-0 [arXiv:1912.12086 [hep-ph]].
- [68] A. C. Aguilar, M. N. Ferreira, C. T. Figueiredo and J. Papavassiliou, Phys. Rev. D **100** (2019) no.9, 094039 doi:10.1103/PhysRevD.100.094039 [arXiv:1909.09826 [hep-ph]].
- [69] M. Vujanovic and T. Mendes, Phys. Rev. D **99** (2019) no.3, 034501 doi:10.1103/PhysRevD.99.034501 [arXiv:1807.03673 [hep-lat]].
- [70] A. Sternbeck, P. H. Balduf, A. Kızılersu, O. Oliveira, P. J. Silva, J. I. Skullerud and A. G. Williams, PoS **LATTICE2016** (2017), 349 doi:10.22323/1.256.0349
- [71] J. de Boer, K. Skenderis, P. van Nieuwenhuizen and A. Waldron, Phys. Lett. B **367** (1996), 175-182 doi:10.1016/0370-2693(95)01455-1 [arXiv:hep-th/9510167 [hep-th]].
- [72] J. Serreau and U. Reinosa, EPJ Web Conf. **137** (2017), 07024 doi:10.1051/epjconf/201713707024
- [73] J. Maelger, U. Reinosa and J. Serreau, Phys. Rev. D **97** (2018) no.7, 074027 doi:10.1103/PhysRevD.97.074027 [arXiv:1710.01930 [hep-ph]].
- [74] J. Maelger, U. Reinosa and J. Serreau, Phys. Rev. D **98** (2018) no.9, 094020 doi:10.1103/PhysRevD.98.094020 [arXiv:1805.10015 [hep-th]].
- [75] N. V. Smolyakov, Theor. Math. Phys. **50** (1982) 225-228 <https://doi.org/10.1007/BF01016449>
- [76] A. I. Davydychev, P. Osland and L. Saks, JHEP **08** (2001), 050 doi:10.1088/1126-6708/2001/08/050 [arXiv:hep-ph/0105072 [hep-ph]].
- [77] A. Weber and P. Dall'Olivo, EPJ Web Conf. **80** (2014), 00016 doi:10.1051/epjconf/20148000016
- [78] J. S. Ball and T.-W. Chiu, Phys. Rev. D **22** (1980) 2550-2557
- [79] S. P. Martin and D. G. Robertson, Comput. Phys. Commun. **174** (2006), 133-151 doi:10.1016/j.cpc.2005.08.005 [arXiv:hep-ph/0501132 [hep-ph]].
- [80] A. V. Smirnov, JHEP **10** (2008), 107 doi:10.1088/1126-6708/2008/10/107 [arXiv:0807.3243 [hep-ph]].
- [81] D. Dudal, H. Verschelde, V. E. R. Lemes, M. S. Sarandy, R. Sobreiro, S. P. Sorella, M. Picariello and J. A. Gracey, Phys. Lett. B **569** (2003), 57-66 doi:10.1016/j.physletb.2003.07.019 [arXiv:hep-th/0306116 [hep-th]].
- [82] N. Wschebor, Int. J. Mod. Phys. A **23** (2008), 2961-2973 doi:10.1142/S0217751X08040469 [arXiv:hep-th/0701127 [hep-th]].
- [83] M. Tissier and N. Wschebor, Phys. Rev. D **79** (2009), 065008 doi:10.1103/PhysRevD.79.065008 [arXiv:0809.1880 [hep-th]].
- [84] J. A. Gracey, Phys. Lett. B **552**, 101-110 (2003) doi:10.1016/S0370-2693(02)03077-0 [arXiv:hep-th/0211144 [hep-th]].